Synthesis and Modeling of Metallic Nanoparticles in Compressed Liquid and Supercritical Fluid Based Reverse Micelles

Christopher B. Roberts*, Christopher L. Kitchens, M. Chandler McLeod
Department. of Chemical Engineering, Auburn University, Alabama USA
* email: croberts@eng.auburn.edu fax: (334) 844-2036

The water/AOT/liquid alkane reverse micelle system has proven to be an effective medium for the production of nanoscale materials and has become a popular area of study. It has been demonstrated that the properties of the bulk alkane phase influence the synthesis of metallic nanoparticles, particularly the ultimate particle size. The use of supercritical fluids as the bulk phase provide a novel medium for particle synthesis in that the properties that control the particle growth can be fine tuned by adjusting the temperature and pressure of the system. In this paper we discuss the properties of the bulk fluid phase and their effects on the synthesis of copper and silver nanoparticles with emphasis on compressed propane and supercritical ethane. The experimental results are complemented by the use of a total interaction energy model used to predict the ultimate particle size produced.

INTRODUCTION

An increasingly popular method for the production of metallic and inorganic nanoparticles employs water-in-oil microemulsion media or reverse micelles as nano-reactors for aqueous phase reactions. This technique has been implemented in liquid solvents for the formation of a variety of materials ranging from semiconductor materials to metallic particles [1-5]. Recently we have extended the application of reverse micelle systems to controlled particle synthesis in compressed and supercritical fluid solvents (SCF) [6, 7]. Despite the extensive use of this technology there has been far less work done in attempt to completely understand the underlying factors that control the nanoparticle growth process. Previous studies have shown that the main factors controlling the growth and resulting particles are the intermicellar interactions, solvent effects, reagent concentrations, and water content of the reverse micelles or W (W=[H_2O]/[AOT]) [4, 8-10]. It has also been shown that the particle growth rates are controlled by the intermicellar exchange rates, which are largely influenced by the thermophysical properties of the bulk fluid [8, 10-13]. We have reinforced this conclusion with our studies of copper and silver nanoparticle formation in various liquid and compressed alkanes as well as supercritical ethane and CO2. The compressed and SCF solvents have shown to be an interesting media where by simply adjusting the pressure or temperature, one can fine-tune the solvent properties thus controlling the particle growth. Recent work has also shown that the bulk solvent strength controls the maximum particle size that the reverse micellar system can support [14]. This becomes increasingly significant when applied to SCF solvents where the maximum particle size becomes a function of the temperature and pressure.

The work presented here provides insight into metallic nanoparticle growth through both experimental and theoretical work in order to gain a better understanding of synthesis in the reverse micelle system. In recent work we have shown that the mean ultimate particle size obtained from synthesis within the liquid reverse micelle system is dependant on the AOT tail / solvent interaction and can be predicted by an interaction energy model [14]. Recent work by Shah et. al. takes an experimental and modeling approach to

successfully describe the dispersion of silver and gold nanoparticles coated with a dodecanethiol ligand within SCF ethane [15]. They demonstrate how a size selective dispersion of nanoparticles can be achieved in SCF ethane by tuning the temperature and pressure thereby controlling the solvent interactions with the dodecane tail of the thiol ligand. We have applied this modeling technique to the study of copper particle production in compressed propane and SCF ethane. Here the surfactant AOT acts as a stabilizing ligand to support an ultimate particle size achieved during synthesis depending on the interaction of the AOT tails with the compressible fluid. This method differs from liquid synthesis, where the solvent properties are tuned by adjusting the temperature and pressure thus providing variation in the ultimate particle size produced.

Model

The model presented here takes a soft sphere approach to model the interactions of metallic nanoparticles coated with AOT surfactant through a bulk fluid. The results of the model are represented by the total interaction energy, equation 1, which is the balance of the van der Waals attraction between particles and the steric repulsion forces due to overlapping of the surfactant tails, each of which are presented as a function of the particle separation distance, h. The repulsive energy contribution consists of an osmotic term, Φ_{osm}, and an elastic term, Φ_{elas}.

$$\Phi_{total} = \Phi_{vdW} + \Phi_{osm} + \Phi_{elas} \tag{1}$$

The van der Waals attractive force, Φ_{vdW}, between two nanoparticles is a function of the particle radius R, the center to center separation d, and the Hamaker constant A_{131}.

$$\Phi_{vdW} = -\frac{A_{131}}{6}\left[\frac{2R^2}{d^2-4R^2} + \frac{2R^2}{d^2} + \ln\left(\frac{d^2-4R^2}{d^2}\right)\right] \quad \text{where} \quad A_{131} \approx \left(\sqrt{A_{11}} - \sqrt{A_{33}}\right)^2 \tag{2}$$

A_{131} is a proportionality factor that accounts for two nanoparticles of the same material (component 1) interacting through a solvent (component 3) and is determined from pure component values. The Hamaker constant for copper and silver nanoparticles are A_{11} = 1.723 eV and 2.440 eV respectfully [16]. The Hamaker constant for the bulk fluid A_{33} is calculated on the basis of Lifshitz theory [17] as a function of the dielectric constant, ε, and the refractive index, n which are calculated from the Clausius-Mossotti relation [18].

The repulsive contribution to the total interaction energy originates from the "soft sphere" theory [15, 19] where equations 3-6 are proposed for the osmotic and elastic terms. The osmotic repulsion term Φ_{osm}, calculated from equations 3 and 4, accounts for the solvent – tail and tail – tail interactions and is a strong function of the Flory-Huggins interaction parameter, χ, which is determined by the Hildebrand solubility parameters of the solvent and the AOT tails. The solubility parameter for the solvent is related to the cohesive energy density and can be calculated from the thermodynamic properties of the system. The solubility parameter for AOT must be estimated using a group contribution method typically implemented for polymer solutions where a molar attraction constant is assigned for each chemical group in the surfactant tail. There are several group contribution methods available including those provided by Small, Hoy, and van Krevelen resulting in values of 517.52, 510.81 and 578.42 $(MPa)^{1/2}$ respectfully [20]. In this case an average of the three methods was implemented to obtain δ_2 = 535.32 $(MPa)^{1/2}$. The elastic repulsion term Φ_{elas}, calculated from equation 5, contributes to the interaction energy in the range $h < l$ and represents the energy requirement for compression of the surfactant tails where l is the AOT tail length.

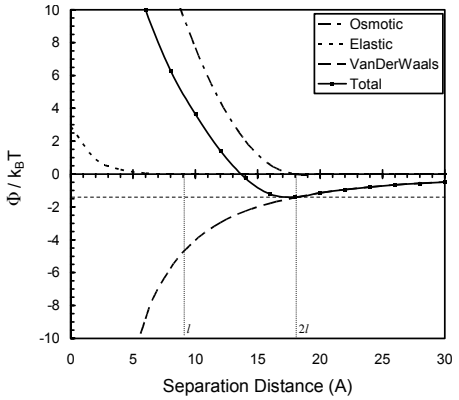

Figure 1. Contributions to the Total Interaction Energy Model for silver nanoparticles coated with AOT dispersed in hexane at 25°C and 1 bar.

$$\Phi_{osm} = \frac{4\pi R k_B T}{v_{solv}} \phi^2 \left(\frac{1}{2} - \chi\right)\left(l - \frac{h}{2}\right)^2 \quad l < h < 2l \qquad (3)$$

$$\Phi_{osm} = \frac{4\pi R k_B T}{v_{solv}} \phi^2 \left(\frac{1}{2} - \chi\right)\left[l^2\left(\frac{h}{2l} - \frac{1}{4} - \ln\left(\frac{h}{l}\right)\right)\right] \quad h < l \qquad (4)$$

$$\Phi_{elas} = \frac{2\pi R k_B T l^2 \phi \rho}{MW_2}\left\{\frac{h}{l}\ln\left[\frac{h}{l}\left(\frac{3-h/l}{2}\right)^2\right] - 6\ln\left(\frac{3-h/l}{2}\right) + 3\left(1 - \frac{h}{l}\right)\right\}$$

$$h < l \qquad (5)$$

$$h = d - 2R \qquad (6)$$

The contribution of each of the terms can be seen in Figure 1 as a function of the separation distance of the particles. The elastic term does not contribute greatly and it is the osmotic forces that control the particle dispersion by countering the attractive van der Waals forces. Along the total interaction energy curve a minimum value will occur at a particular separation distance which is compared to an energy of -3/2 $k_B T$ required to disperse the particles within the bulk solvent. Particle growth occurs through random exchange of micelle contents and will continue to grow until this limit is reached. If growth beyond this limit occurs, the particles will precipitate out of solution. On the other hand, if the repulsive terms are insufficient to balance the attractive forces flocculation will occur preventing any particle growth. The total interaction energy can be calculated as a function of the separation distance for various particle sizes, solvents, temperatures and pressures in order to determine the optimum operating conditions for particle growth.

EXPERIMENTAL

Materials Sodium bis(2-ethylhexyl) sulfosuccinate (AOT) and DIUF Water were obtained from Fisher Scientific and used without further purification. Ethane and Propane gases were purchased from BOC Gases and were passed through a High Pressure Gas Drier moisture trap and a High Pressure Oxy-Trap oxygen trap, both purchased from Alltech. Anhydrous Hydrazine 98%, Isooctane, and other alkane solvents were purchased from Sigma Aldrich. The alkane solvents were stored over molecular sieves to remove any dissolved water. Copper AOT ($CuAOT_2$) was synthesized by two separate methods published previously [21, 22] where the sodium ion of the AOT headgroup was replaced by a Cu^{2+} ion to create the functionalized surfactant.

Particle Synthesis Methods for the synthesis of copper nanoparticles via. $CuAOT_2$ reduction using hydrazine within a liquid phase AOT reverse micelle system have been discussed in previous literature [8]. Particle synthesis in compressed propane and SCF ethane were achieved in a 90 ml stainless steel reactor fitted with two opposing quartz windows for UV-vis absorption measurements. The reactor was accessorized with HiP fittings for an inlet and outlet, an RTD temperature controller, an Omega digital pressure gauge, and a Valco Instruments six port injection loop. AOT and $CuAOT_2$ were added to the reactor in a 10 to 1 ratio and the vessel was then sealed, purged with nitrogen gas and evacuated by a vacuum pump. The purging and evacuation was performed two additional

times to ensure an oxygen free environment and prevent the formation of copper oxide. The reactor was then filled with the bulk compressed fluid using an ISCO 260D high pressure syringe pump and simultaneously the injection loop was used to introduce the desired amount of water for a W = 5 or less (W = $[H_2O]/[AOT]$). The reactor pressure was brought to 100 bar at the desired temperature for the reaction. Hydrazine (3 X $[CuAOT_2]$) was then added via the injection loop and the system was brought to the desired reaction pressure. The reactor was then placed in the Varian Cary 300 UV-Vis spectrophotometer and the time resolved absorbance measurements were recorded as the reaction proceeded.

Particle images were obtained using a Zeiss EM 10 Transmission Electron microscope (TEM). The particles were collected by either depressurizing and spraying the particles through a 100 μm capillary tube onto a nickel TEM grid or by redispersion in ethanol and placing a droplet of the solution on the TEM grid.

RESULTS AND CONCLUSIONS

We have previously shown [14] that the total interaction energy model was able to predict the ultimate particle size obtained in liquid reverse micelle systems. For copper nanoparticles, the ultimate particle sizes obtained ranged from 9 nm to 12 nm depending on the bulk solvent used which ranged from pentane to dodecane for n-alkanes as well as isooctane and cyclohexane. The model was also used to predict that the ultimate particle size for silver synthesis in hexane would be approximately 7 nm diameter particle. Figure 2 shows the results from the model where the total interaction energy, Φ_{tot}/k_BT is plotted as a function of separation distance and particle size for silver nanoparticles ranging in diameter from 6 nm to 12 nm, coated with AOT surfactant and dispersed in n-hexane at 25°C and 1 bar. From the energy curves a minimum value is observed and when this minimum energy value is compared with an energy of -3/2 k_BT required to disperse the particles within the bulk solvent we find that a 7 nm diameter silver particle can be stericly supported in solution while a 8 nm or larger particle can not be supported. This would lead us to believe that the silver nanoparticles synthesized in a Hexane/AOT/Water reverse micelle system would be on the order of 7 nm in diameter. Results from TEM analysis of silver nanoparticles obtained from a hexane solution with [AgAOT] = 0.001M, [AOT] = 0.099M, and W = 10 are presented in Figure 3 where the majority of the silver nanoparticles are 6 to 7 nm in diameter, corresponding directly to the predictions of the model.

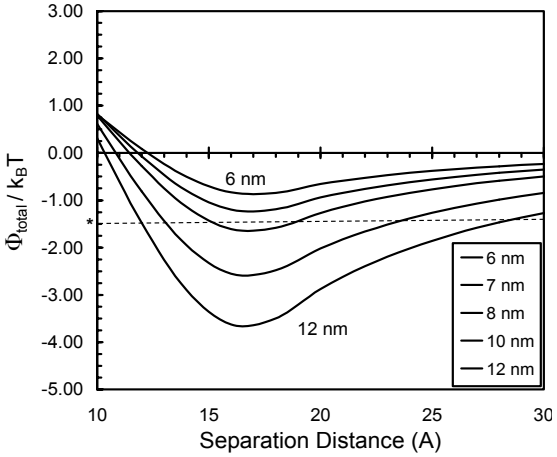

Figure 2. Plot of the Φ_{total}/RT curves calculated for 6nm to 12nm diameter Ag nanoparticles coated with AOT and dispersed in hexane at 25°C and 1 bar.

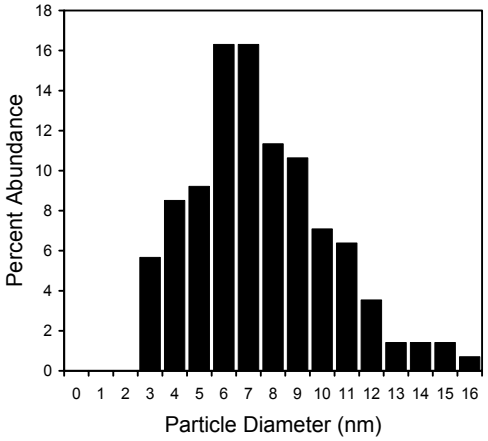

Figure 3. Size distribution for Ag particles synthesized in liquid hexane–AOT– water reverse micelle system with $1.0x10^{-3}$ M AgAOT, $9.9x10^{-2}$ M AOT, and W = 10.

Solvent	Particle Diameter (nm)	Pressure (bar)	Temperature (°C)	[$CuAOT_2$] (mol/dm^3)	[AOT] (mol/dm^3)	W
Propane	9.1	310	23	5.53×10^{-3}	5.53×10^{-2}	5
Propane	6.3	255	23	5.53×10^{-3}	5.53×10^{-2}	5
SCF Ethane	-	400	37	5.53×10^{-3}	5.53×10^{-2}	-
SCF Ethane + 14% Isooctane	9.1	245	37	5.00×10^{-3}	5.00×10^{-2}	7.8
Liquid Isooctane	13.0	1	37	8.00×10^{-2}	5.00×10^{-1}	7

Table 1. Cu particle sizes synthesized in compressed propane, SCF ethane/isooctane mixture, and isooctane above the ethane critical temperature. Synthesis in SCF ethane solvent was not achieved.

The study of particle formation in liquid solvents has demonstrated that the bulk solvent properties have an effect on the ultimate particle size obtained by reverse micellar synthesis. SCF solvents offer the unique ability to adjust their solvent strength by simply changing the temperature or pressure. When the total interaction energy model is applied to the compressed propane – AOT – copper nanoparticle system in Figure 4, we see that the ability to support copper nanoparticles increases with an increase in pressure. Figure 4a shows that in propane there is a minimum pressure of 350 bar required to support a 10 nm diameter particle at 25°C. Theoretically, pressures below this value causes the Φ_{tot}/k_BT curve to fall below the -3/2 k_BT interaction energy limit and a 10 nm diameter particle can not be formed below 350 bar. Temperature effects are also predicted by the model where a decrease in temperature allows for the formation of larger particles. Figure 4b shows the effect of particle size on Φ_{tot}/k_BT in compressed propane at 25°C and 310 bar where a particle with 9 nm diameter would be supported and theoretically a 10 nm diameter particle would not be formed. Table 1 reveals that particle synthesis in compressed propane with W=5 at 23°C and 310 bar results in the formation of 9.1 nm diameter copper particles which corresponds directly to the particle size predicted in the model from Figure 4b. Table 1 also shows that particle formation under similar condition at 255 bar results in copper particles with a diameter of 6.3 nm, thus supporting the model where a lower pressure results in the formation of a smaller particle.

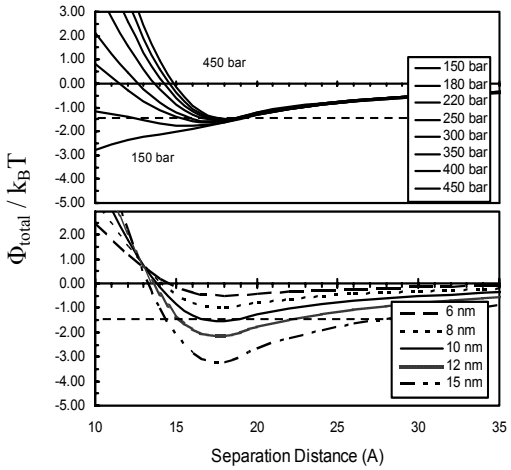

Figure 4. Plot of the Φ_{total}/RT curves for Cu nanoparticles coated with AOT and dispersed in compressed propane at 25°C. **4a)** shows the effects of pressure on 10nm diameter Cu particles in the range of 150 to 450 bar. **4b)** Shows the effect of particle diameter from 6nm to 15 nm at 310 bar.

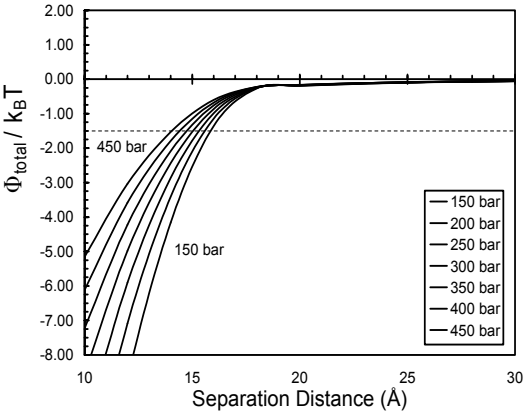

Figure 5. Plot of the Φ_{total}/RT curves for 4nm diameter Cu nanoparticles coated with AOT and dispersed in SCF ethane at 35°C and pressures from 150 to 450 bar. The graph demonstrates the inability to synthesize Cu particle in SCF ethane.

When the total interaction energy model is applied to the SCF ethane – AOT – copper nanoparticles system we find that under reasonable operating conditions (pressures up to 450 bar) the solvent – tail interactions are not favorable enough to support the formation of copper particles of any size. Figure 5 shows that in SCF ethane at 35°C copper particles 4 nm in diameter can not be supported and this corresponds to the inability to synthesize copper nanoparticles in the SCF ethane system experimentally. However, with the addition of 14 % (v/v) isooctane cosolvent the properties of the bulk solvent are adjusted to create a more favorable solvent – tail interaction thus allowing for the formation of copper nanoparticles. From Table 1 copper nanoparticals 9.1 nm in diameter are synthesized in a SCF ethane / isooctane mixture at 37°C and 245 bar with W=7.8 [7]. This particle size can be compared to copper nanoparticles 13 nm in diameter obtained from synthesis in pure isooctane with the same surfactant concentrations and W=7 at 37°C and we find that the presence of SCF ethane decreases the favorable solvent – tail interaction thus resulting in a smaller ultimate particle size.

ACKNOWLEDGEMENTS

The authors would like to gratefully acknowledge financial support from the Department of Energy – Basic Energy Sciences (DE-FG02-01ER15255).

REFERENCES

1. Pileni, M.P., Langmuir, Vol. 13(13), **1997**, p. 3266.
2. Eastoe, J., Warne, B., Curr. Opin. Colloid Interface Sci., Vol. 1(6), **1996**, p. 800.
3. Wu, M.L., Chen, D.H., Huang, T.C., Langmuir, Vol. 17(13), **2001**, p. 3877.
4. Hirai, T., Sato, H., Komasawa, I., Ind. Eng. Chem. Res., Vol. 33(12), **1994**, p. 3262.
5. Towey, T.F., Khanlodhi, A., Robinson, B.H., J. Chem. Soc. Faraday Trans., Vol. 86(22), **1990**, p. 3757.
6. Cason, J.P., Roberts, C.B., J. Phys. Chem. B, Vol. 104(6), **2000**, p. 1217.
7. Cason, J.P., Khambaswadkar, K., Roberts, C.B., Ind. Eng. Chem. Res., Vol. 39(12), **2000**, p. 4749.
8. Cason, J.P., Miller, M.E., Thompson, J.B., Roberts, C.B., J. Phys. Chem. B, Vol. 105(12), **2001**, p. 2297.
9. Lisiecki, I., Pileni, M.P., J. Phys. Chem., Vol. 99(14), **1995**, p. 5077.
10. Bagwe, R.P., Khilar, K.C., Langmuir, Vol. 16(3), **2000**, p. 905.
11. Eicke, H.F., Shepherd, J.C.W., Steinemann,. A., J. Coll. Interface Sci., Vol. 56(1), **1976**, p. 168.
12. Fletcher, P.D.I., Howe, A.M., Robinson, B.H., J. Chem. Soc. Faraday Trans., Vol. 83, **1987**. p. 985.
13. Atik, S.S., Thomas, J.K., J. Am. Chem. Soc., Vol. 103(12), **1981**, p. 3543.
14. Kitchens, C.L., McLeod, M.C., Roberts, C.B., Submitted to J. Phys. Chem B, **2003**.
15. Shah, P.S., Holmes, J. D., Johnston, K. P., Korgel, B. A., J. Phys. Chem. B, Vol. 106(10), **2002**, p. 2545.
16. Eichenlaub, S., Chan, C., Beaudoin, S.P., J. Coll. Interface Sci., Vol. 248(2), **2002,** p. 389.
17. Israelachvili, J.N., *Intermolecular and Surface Forces*, 2nd ed.; Academic Press.: New York, **1985**.
18. Younglove, B.A., Ely, J.F., J.f Phys. Chem. Ref. Data, Vol. 16(4), **1987**, p. 577.
19. Vincent, B., Edwards, J.,Emmett, S., Jones, A., Colloids and Surfaces, Vol. 18(2-4), **1986**, p. 261.
20. Fried, J.R., *Polymer Science and Technology*, Prentice Hall, Englewood Cliff, NJ, **1995**.
21. Eastoe, J., Fragneto, G., Robinson, B. H., Towey, T. F., Heenan, R. K., Leng, F. J., J. Chem. Soc. Faraday Trans., Vol. 88(3), **1992**, p. 461.
22. Petit, C., Lixon, P., Pileni, M.P., J. Phys. Chem., Vol. 94(4), **1990**, p. 1598.